PHYSICAL REVIEW B VOLUME 45, NUMBER 10 1 MARCH 1992-II

Atomic volumes of rare-earth metals under pressures to 40 GPa and above

W. A. Grosshans* and W. B. Holzapfel
Fachbereich Physik, Universität-GH-Paderborn, Postfach 16 21, D-4790 Paderborn, Germany

(Received 28 May 1991; revised manuscript received 16 September 1991)

High-pressure studies on most of the rare-earth metals using diamond anvil cells and energy-dispersive x-ray diffraction with either a conventional x-ray source or synchrotron radiation are presented, together with a systematic comparison of the results on the equations of state. This comparison leads to simple scaling relations for the regular rare-earth metals and to distinct deviations for the anomalous or "collapsed" phases.

INTRODUCTION

The rare-earth metals (RE) represent a family of elements with a large group of "regular" members with very similar properties and a small group consisting of the three "irregular" members, Ce, Eu, and Yb, which show some interesting anomalies in most of their physical properties. Aspects of systematics in the structural phase transitions for all the regular RE under pressure have been reviewed just recently.[1] As part of such studies, detailed equation of state (EOS) data for all these elements were also obtained at room temperature in a largely extended range of pressure[2,3] suitable for a systematic intercomparison with previous and recent data[4–45] obtained either with isothermal direct volume or x-ray diffraction techniques[3–35] or with adiabatic ultrasonic or shock-wave measurements.[34–45] Finally, the use of a recently proposed method[46–48] for the evaluation of such data elucidates some correlations between details in EOS data and changes in the electronic structure within the present experimental range of pressures.

EXPERIMENTAL TECHNIQUE

The present experiments made use of a diamond anvil cell[49,50] and energy-dispersive x-ray diffraction device[1–3,50–53] using either a conventional x-ray source with a conical slit system[50–52] or synchrotron radiation with conventional diffraction geometry[53] when higher resolution was required. Pressures were determined with the ruby luminescence technique[54–58] and the nonlinear ruby pressure scale.[58] Deviatoric stresses and pressure gradients were minimized by the use of liquid (or solid) nitrogen as the pressure-transmitting medium.[53] The sample materials were provided by Gschneidner, together with detailed chemical analyses, which have been tabulated previously.[1] In short, H and O represented the dominant impurities, typically with atomic concentrations between 200 and 500 ppm but in a few cases (Eu and Tm) at a level of up to 2600 ppm. Impurity levels from other metals or other RE elements on the other hand were generally much below 100 ppm.

EXPERIMENTAL RESULTS

The original spectra, as well as details of the evaluation of these spectra, have not been reproduced here since many examples have been given previously together with the structural analyses.[1,3] These detailed evaluations showed that the lattice parameters are determined typically with a precision of better than 1×10^{-3} even for the orthorhombic or trigonal structures.

Calibration measurements with NaCl, Ag, and ruby luminescence sensors for increasing as well as decreasing pressures indicated that the dominant uncertainties resulted not from these lattice parameter determinations but from uncertainties in the average pressure due to pressure gradients between the ruby sensor locations and the sample. Typically, these uncertainties generated a scatter of the data around the smoothed EOS curves with a mean deviation of less than ±1 GPa. Nevertheless, a scatter or systematic deviations of more than 2 GPa could sometimes be observed just in the upper pressure range. This scatter as well as comparisons with previous data are illustrated in Figs. 1 to 15, where the solid curves represent least-squares fitted EOS curves of the Murnaghan type[61] according to the form

$$p=p_r+(K_r/K_r')[(V_r/V)^{K_r'}-1] .$$

Thereby, p_r and V_r stand for the pressure and volume at a fixed reference point and the two adjustable parameters K_r and K_r' are usually supposed to represent the bulk modulus and its pressure derivative at this fixed point. This interpretation of the parameters K_r and K_r' requires however that the EOS data are reproduced in every detail by such a smooth analytic form.

The detailed comparison with ultrasonic data given on Table I may cast some doubt on the validity of this interpretation of the parameters K_r and K_r' in general and therefore, these parameters should be considered here at first only as best-fitted values for a specific EOS form. For ambient pressure phases, the common choice for the parameters p_r and V_r is $p_r=p_0=100$ kPa and $V_r=V_0$ which represents than the volume at ambient condition. For high pressure phases, however, the corresponding value of V_0 is usually not known and therefore either this value V_0 or V_r at any other arbitrarily selected value p_r must than be treated as the third adjustable parameter in the fitting procedure.

For a direct comparison with previous data, the present results are plotted at first in the usual way as shown in Figs. 1 to 15. In general, the agreement with previous static data for the lower pressure range is reasonable and, usually, the agreement with the shock-wave data for the higher pressure range is even better. Systematic deviations between the present data and the earlier shock-wave results are noticed, however, for Pr and Eu, and it is quite likely that the thermal corrections used in the reduction of the shock-wave data can account for these discrepancies since also the thermal properties

TABLE I. Intercomparison of adiabatic (*S*) and isothermal (*T*) data for K_0 and K'_0 given in the literature (Refs. 3–45) together with the highest pressures p_m limiting the pressure range in the various isothermal measurements. The last line for each of the lanthanide elements gives the "average" values according to Eq. (1) for "normal" trivalent behavior. These "normal" values are placed in parentheses to indicate anomalous behavior when the experimental values deviate significantly.

R	K_0 (GPa)	K'_0	p_m (GPa)	Ref.	
La	30			*S*	34
	28			*S*	39
	24				35
	24	5.0	10	*T*	5
	25			*T*	34
	25	3.2	5	*T*	11
	25	2.8	12	*T*	15
	22	3.9	40	*T*	3
	23	(2.9)	20	*T*	av.
Ce	20			*S*	34
	24				35
	20			*T*	5
	21			*T*	34
	(28)	(2.9)	20	*T*	av.
Pr	30			*S*	34
	30			*S*	39
	29			*S*	41
	29	4.3		*S*	43
	31				35
	26	5.2	10	*T*	5
	37	8.0	5	*T*	6
	28			*T*	34
	30	1.6	5	*T*	12
	28	2.1	20	*T*	3
	28	(2.9)	20	*T*	av.
Nd	33			*S*	34
	33			*S*	39
	32			*S*	42
	32	4.4		*S*	43
	33				35
	31	4.5	10	*T*	5
	32			*T*	34
	33	3.0	5	*T*	12
	28	2.7	40	*T*	3
	30	2.9	20	*T*	av.
Pm	38	1.5	60	*T*	22
	31	2.9	20	*T*	av.
Sm	38			*S*	34
	37			*S*	39
	29				35
	27	6.0	4	*T*	5
	28			*T*	34
	27	2.8	38	*T*	3
	31	2.5	100	*T*	23
	33	2.9	20	*T*	av.
Eu	17			*S*	39
	12				35
	13	3.0	5	*T*	6
	12	2.8	2	*T*	8
	12	2.8	10	*T*	10
	12	3.0	27	*T*	33
	12	2.3	12	*T*	3
	(18)	(2.9)	20	*T*	av.
Gd	39			*S*	34
	39			*S*	39
	38	3.3	1	*S*	40
	38				35
	36	6.0	4	*T*	5
	39			*T*	34
	36	4.8	5	*T*	12
	34	3.2	21	*T*	33
	37	2.3	57	*T*	3
	23	4.3	106	*T*	21
	35	2.9	20	*T*	av.
Tb	40			*S*	34
	40			*S*	37
	39	2.4		*S*	43
	40				35
	46	2.0	5	*T*	6
	40		3	*T*	8
	37	2.7	42	*T*	20
	41	2.5	58	*T*	3
	38	2.9	20	*T*	av.
Dy	41			*S*	34
	41	3.2	1	*S*	40
	41			*S*	39
	39				35
	34	7.0	4	*T*	5
	38			*T*	34
	40	5.1	5	*T*	12
	39	2.8	47	*T*	3
	40	2.9	20	*T*	av.
Ho	46			*S*	34
	43	2.8		*S*	43
	40				35
	39			*T*	34
	37	6.0	4	*T*	5
	33	5.0	20	*T*	9
	46	2.2	44	*T*	3
	42	2.9	20	*T*	av.
Er	45			*S*	34
	45	3.3	1	*S*	40
	46	3.3		*S*	43
	41				35
	37	6.0	4	*T*	5
	39			*T*	34
	39	6.0	20	*T*	9
	45	3.5	5	*T*	12
	41	2.9	30	*T*	3
	44	2.9	20	*T*	av.
Tm	40	4.3		*S*	43
	40				35
	37	7.0	4	*T*	5
	38			*T*	34
	40	4.3	19	*T*	9
	45	2.3	42	*T*	3
	46	2.9	20	*T*	av.
Yb	14			*S*	34
	15			*S*	39
	13				35
	17		4	*T*	4
	12	3.4	4	*T*	5
	14	3.5	4	*T*	6
	13			*T*	34
	14	3.2	34	*T*	33
	(28)	(2.9)	20	*T*	av.
Lu	48			*S*	38
	48	3.3		*S*	43
	41				35
	39	5.0	4	*T*	5
	42			*T*	34
	46	2.8	20	*T*	16
	49	2.9	42	*T*	3
	50	2.9	20	*T*	av.
Sc	55			*S*	39
	57	3.1		*S*	43
	43				35
	60	5.0	5	*T*	6
	44		2	*T*	8
	60	2.8	20	*T*	3
Y	42			*S*	36
	50			*S*	39
	37	3.3		S	43
	37				35
	34	5.0	4	*T*	5
	40	2.4	50	*T*	3

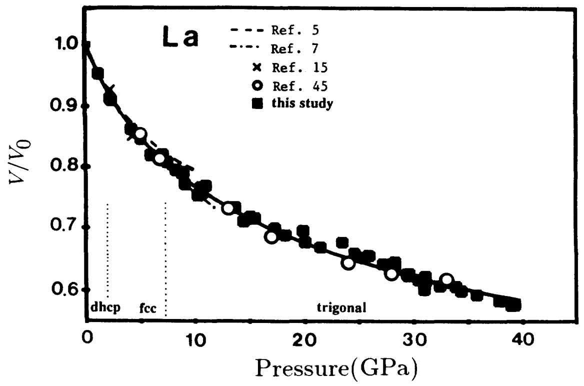

FIG. 1. Isothermal (room-temperature) pressure-volume data for La from this study compared with previous results (Refs. 5, 7, 15, and 45).

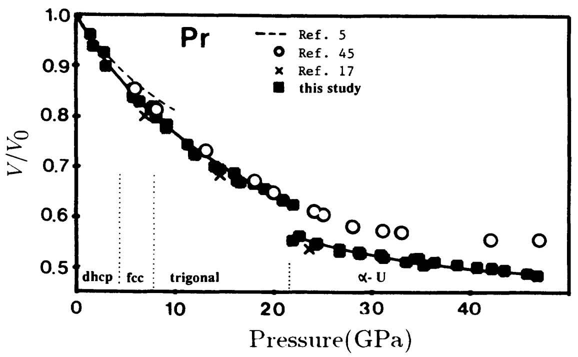

FIG. 2. Isothermal (room-temperature) pressure-volume data for Pr from this study compared with previous results (Refs. 5, 17, and 45). The data of Ref. 17 for the phase Pr IV are rescaled according to the α-U indexing proposed in Refs. 18 and 19.

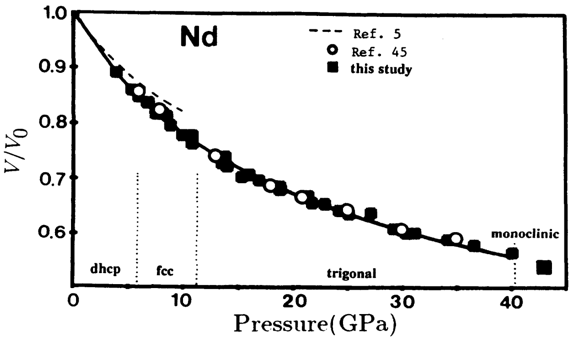

FIG. 3. Isothermal (room-temperature) pressure-volume data for Nd from this study compared with previous results (Refs. 5 and 45).

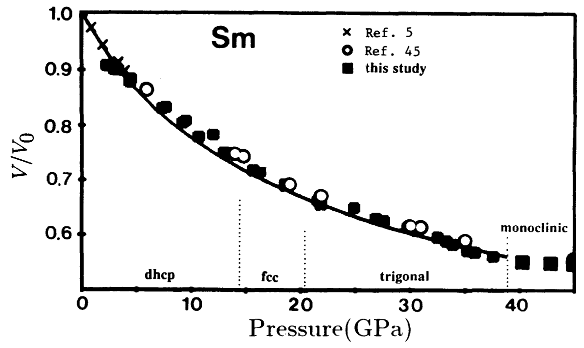

FIG. 4. Isothermal (room-temperature) pressure-volume data for Sm from this study compared with previous results (Refs. 5 and 45). The more recent data of Ref. 20 extending to higher pressures are compared with the present data in Fig. 16.

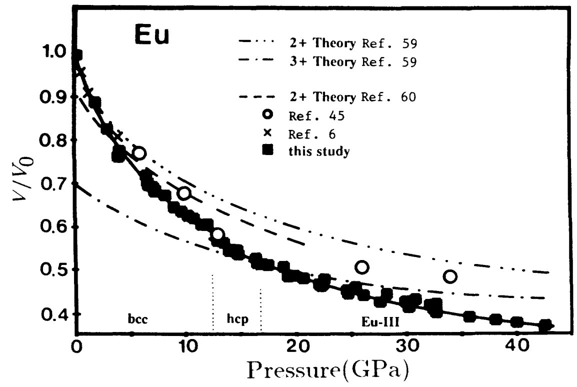

FIG. 5. Isothermal (room-temperature) pressure-volume data for Eu from this study compared with previous results (Refs. 6, 45, 59 and 60). Data of McWhan *et al.* (Ref. 10) to 10 GPa and Takemura *et al.* (Ref. 33) to 27 GPa coincide within experimental accuracy with the present data and are therefore not reproduced here.

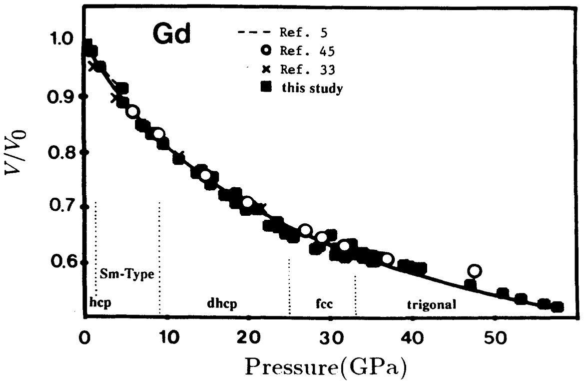

FIG. 6. Isothermal (room-temperature) pressure-volume data for Gd from this study compared with previous results (Refs. 5, 33, and 45). The more recent data of Ref. 21 extending to higher pressures are compared with the present data in Fig. 16.

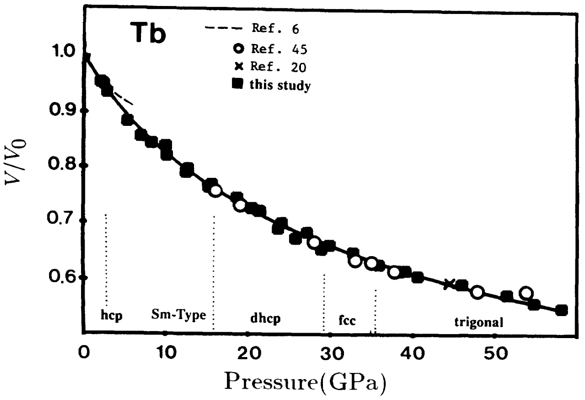

FIG. 7. Isothermal (room-temperature) pressure-volume data for Tb from this study compared with previous results (Refs. 6, 20, and 45).

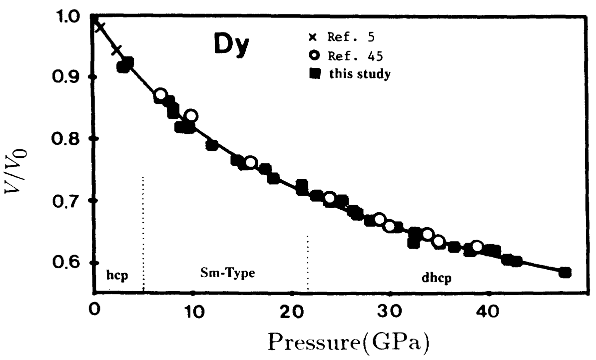

FIG. 8. Isothermal (room-temperature) pressure-volume data for Dy from this study compared with previous results (Refs. 5 and 45).

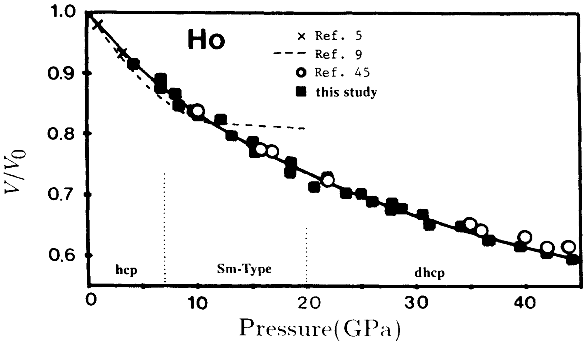

FIG. 9. Isothermal (room-temperature) pressure-volume data for Ho from this study compared with previous results (Refs. 5, 9, and 45).

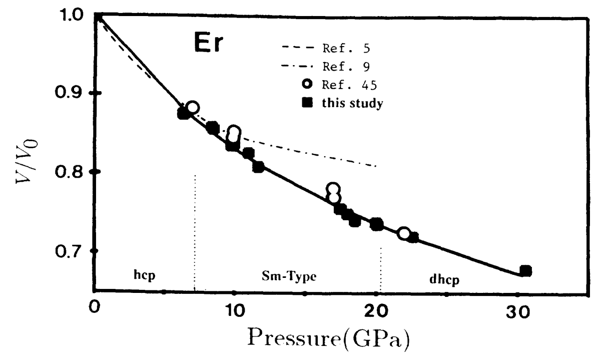

FIG. 10. Isothermal (room-temperature) pressure-volume data for Er from this study compared with previous results (Refs. 5, 9, and 45).

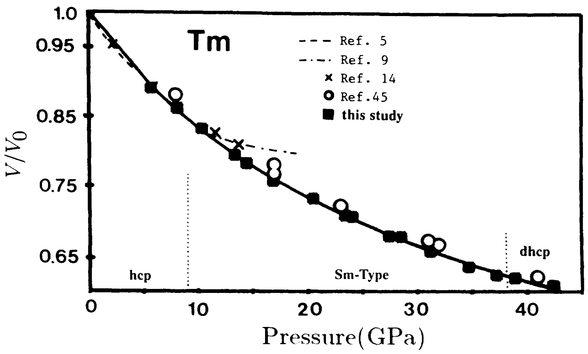

FIG. 11. Isothermal (room-temperature) pressure-volume data for Tm from this study compared with previous results (Refs. 5, 9, 14, and 45).

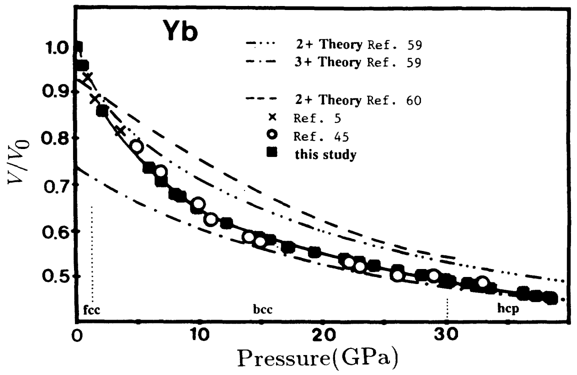

FIG. 12. Isothermal (room-temperature) pressure-volume data for Yb from this study compared with previous results (Refs. 5, 32, 33, 45, 59, and 60). Data of Syassen *et al.* (Ref. 32) to 29 GPa and Takemura *et al.* (Ref. 33) to 34 GPa coincide within experimental accuracy with the present data and are therefore not reproduced here.

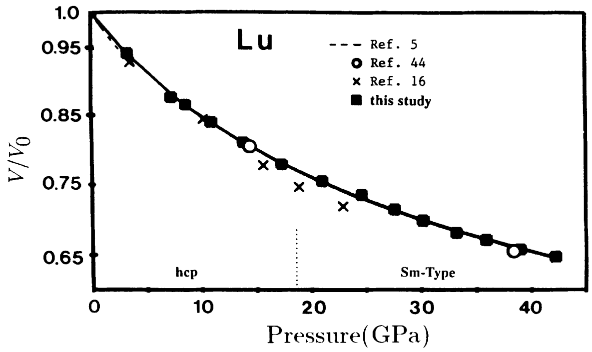

FIG. 13. Isothermal (room-temperature) pressure-volume data for Lu from this study compared with previous results (Refs. 5, 16, and 44).

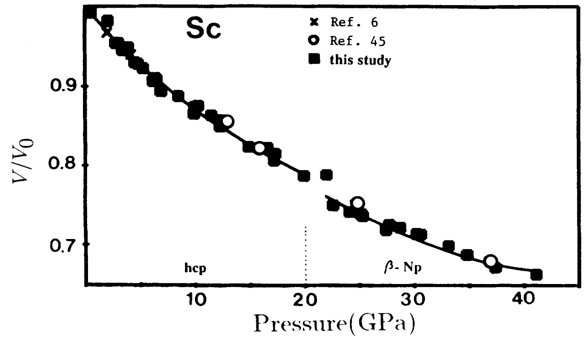

FIG. 15. Isothermal (room-temperature) pressure-volume data for Sc from this study compared with previous results (Refs. 6 and 45).

of Pr and Eu must be considered as anomalous under high pressure.

Since the different structures in the regular RE sequence hcp-(Sm-type)-dhcp-fcc represent only different polytypes with different stacking sequences of hexagonal closed packed layers, it is not astonishing that the small possible volume discontinuities at these (rather sluggish) phase transitions are not discernible at the present level of resolution. Therefore, it appears also reasonable to fit all the EOS data for these "regular" phases with just one common and smooth analytic form over the full pressure range marked under p_m in Table I. This type of a conventional analysis was performed in thesis work of Grosshans[3] and resulted in the values for K_0 and K_0' given in Table I with the reference T 3, where the T stands for isothermal data and 3 gives the reference number. This code with S for adiabatic data and—for unidentified values is also used for the other references[4–42] in Table I to allow for a convenient intercomparison. In the comparison of adiabatic, K_{0S}, and isothermal, K_{0T}, values for the bulk modulus one has to take into account the difference $\Delta K = K_S - K_T = \gamma^2 c_v T/V$ which is typically of the order of 1.5(9)GPa for all the regular lanthanides at ambient condition and can be estimated easily by the use of $\gamma = 1.5(5)$ for the Grüneisen parameter and $c_v = 3k$ for the atomic heat capacity at ambient temperature T with literature values for the atomic volume V. An inspection of Table I shows clearly, that this correction is very small in comparison to the scatter of the values for K_{0T}. Only with respect to the "average" isothermal value given in the last line for each lanthanide with the reference "T av." in Table I, this correction seems to improve the agreement in most of the "regular" cases, though not for Tm and Lu. Since the use of different EOS forms and different pressure ranges as well as the strong (anti)correlation between the parameters K_0 and K_0' in the fitting are responsible for the large scatter in the isothermal values K_{0T}, a special procedure was applied to derive the "average" values in Table I. In fact, it should be noted also that ultrasonic measurements on La and Pr under pressures up to 8.4 GPa (Ref. 62) do not show the smooth increase in $K_S(p)$ implicitly assumed in all the second-order EOS forms commonly in use[46] but rather also some slight oscillatory behavior. Therefore, the fitted EOS parameters, K_{0T} and K_{0T}', from direct volume or x-ray measurements can represent the true variation $K_T(p)$ only when the actual EOS is sufficiently smooth and correctly represented by the analytic form used in the fitting procedure.

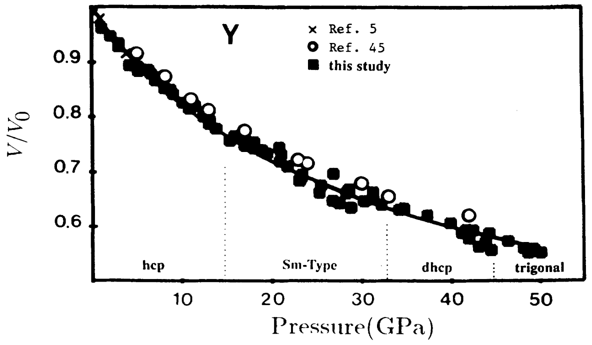

FIG. 14. Isothermal (room-temperature) pressure-volume data for Y from this study compared with previous results (Refs. 5 and 45).

To avoid complications inherent in these fitting procedures, a convenient "linearization" scheme[46–48] is directly applied here to all the experimental data in such a way that the experimental uncertainties as well as the really significant differences between the various data sets are immediately evident as shown in Figs. 16 and 17. In the spirit of a Thomas-Fermi scaling,[63,64,32,46–48] the values $\eta = \ln(p/p_{FG}) - \ln(1-\sigma/\sigma_0)$ are plotted with respect to the atomic length scale $\sigma = (3ZV/4\pi)^{1/3}$ for all the lanthanides in these figures. Thereby, $p_{FG} = a_{FG}(Z/V)^{5/3}$ stands for the pressure of a Fermi gas with the universal parameter $a_{FG} = [(3\pi^2)^{2/3}/5]\hbar^2/m_e = 2.3369$ TPa Å^5 and Z/V represents the mean electron density, when Z is the number of electrons per atom and V the atomic volume.

At first, one may notice that this scaling results in an almost common value $\sigma_0 = 7.92(3)$ Å for all the regular lanthanides at ambient pressure and temperature with small positive deviations for La (7.99 Å), Gd (7.69 Å), and Lu (7.94 Å), Fig. 16, and negative deviations for Ce

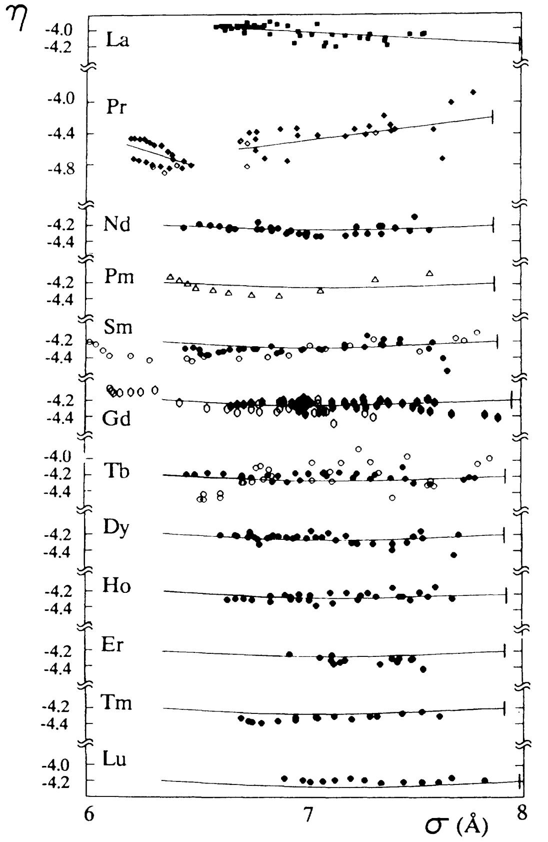

FIG. 16. EOS data for the "regular" lanthanides in η-σ representation with $\eta=\ln(p/p_{\mathrm{FG}})-\ln(1-\sigma/\sigma_0)$ using Thomas-Fermi scaling for the atomic length parameter σ and the Fermi gas pressure p_{FG}. Open symbols refer to recent data from the literature (Refs. 14–23) for this extended pressure range.

(7.81 Å), Fig. 17. While the anomaly for Ce (7.81 Å) is marginal, the divalent elements Eu (8.97 Å) and Yb (8.83 Å) also show here their well-pronounced positive deviations, Fig. 17.

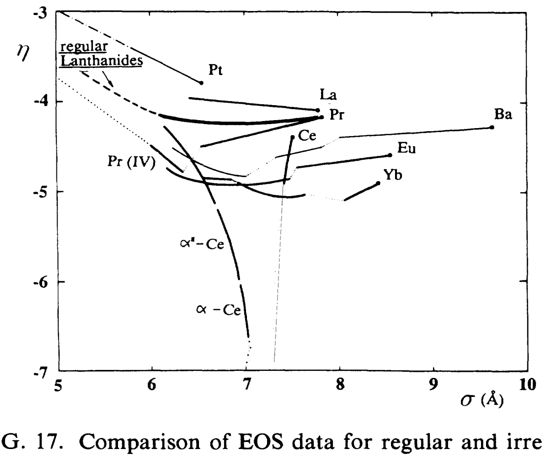

FIG. 17. Comparison of EOS data for regular and irregular lanthanides with "ideal" behavior represented by Pt and with the divalent reference alkali rare earth metal Ba and η-σ representation as in Fig. 16. Data for Pt (Ref. 65), Ba (Refs. 66–68), and Ce (Refs. 24–31) are taken from the literature.

DISCUSSION

If one plots all the data from Fig. 16 just in one diagram on top of each other, as shown in Fig. 17, one can see that most of the high pressure data for the regular lanthanides scatter around a constant value of $\eta=-4.24(8)$ with some significant deviations from this value for La and Pr under pressure. A detailed numerical analysis for all the data in the range 0–20 GPa, and only for the regular lanthanides (excluding La, Ce, Pr, Eu, and Yb), reveals a slightly positive slope $\eta_0'=0.9(9)$ and a common best fitting value $\eta_0=-4.20(7)$ for all these lanthanides at ambient conditions. With the relations[48] for $K_0=(p_{\mathrm{FG}0}/3)\exp\eta_0$ and $K_0'=3-(2/3)\eta_0'$ one obtains then the present "best values" given in Table I in the last line for each lanthanide with the reference "T av." The parentheses around the values for K_0' for La and Pr indicate at these places that the common value of 2.9 does not fit, and individual values have to be taken.

As expected, the adiabatic as well as the isothermal values of K_0 for Ce, Eu, and Yb deviate also significantly from these average values for "normal" behavior and, therefore, the normal values are placed into parentheses also here. Furthermore, the ultrasonic data for Sm seem to deviate in the direction which would correspond to a larger initial value and an anomalously strong negative slope at moderate compression. However, the accuracy of the x-ray data is insufficient to support this observation. The marginal deviations for Pm, Tm, and Lu appear to be still within the experimental uncertainties and the present average isothermal value of K_{0T} for La seems to agree more closely to previous K_{0T} values than to the average from the ultrasonic data $K_{0T}=K_{0S}-1.5(7)\,\mathrm{GPa}=27(2)$ GPa. To summarize these observations we note that the simple relation

$$K_{0T}=1.07(8)Z^{10/3}\sigma_0^{-5}\,\mathrm{GPa}\,\text{Å}^5 \tag{1}$$

fits all the data for the "regular" lanthanides, including La, Pr, Nd, Pm, Sm, Gd, Tb, Dy, Ho, Er Tm, and Lu, within the experimental accuracy. In fact, the scatter in the data for Gd taken from different authors[3,21] is even larger than the differences between the "regular" lanthanides measured just by one group. Furthermore, the relation (1) now gives a quantitative measure for the anomalies in the K_{0T} values of Ce, Eu, and Yb and a weak indication also for a slightly anomalous behavior of Sm at low pressures. In addition to the well-known anomalies of Ce, Eu, and Yb, the data in Fig. 17 reveal also a similarity in the behavior of Ce and Pr under pressure, and furthermore, a weak anomaly for La under pressure, as well as for Sm in its low-symmetry structure[1,3] but not the slightest volume anomaly for the few data points of Nd at the highest pressure in low-symmetry structures.[1,3]

On the other hand, one can compare these data in Fig. 17 also with the behavior of more "ideal" solids,[47,48] such as Ni or Pt (dash-dotted line), and with an approximate lower bound represented by the dotted line, which corresponds to an EOS of the form $p_{MTF}=p_{\mathrm{FG}}(\sigma)\exp(-\beta_0\sigma)(1-\sigma/\sigma_0)$ with the two free parameters β_0 and σ_0 where β_0 is used to fit the leading term in the Thomas-Fermi correction to the pressure p_{FG} of a Fermi gas[47,48] and with the second parameter σ_0 is used to describe the initial value for the "collapsed" phase of Pr. Within these bounds, the extrapolations of the EOS data for the regular lanthanides, as well as for Pr, Ce, Yb, Eu, and La merge into a common curve at very high compression ($\sigma < 5$ Å). However, the behavior of Ba,[66–68] which is often compared with Eu and Yb at moderate pressures, becomes distinctly different in the intermediate pressure range as illustrated by the thin line for Ba, representing available data from the literature.[66–68]

In comparison with the strong increase of η for "regular" solids such as Pt, the weak increase (or even small initial decrease) of η for all the regular lanthanides at moderate compression can be related to the well-known *s-d* electron transfer common to all the heavy group-IA, group-IIA, and early transition metals under pressure.[69–71] The upturn for La and similarly a later upturn for all the other regular lanthanides at stronger compression ($\sigma < 6$ Å) corresponds within this picture just to the completion of this *s-d* electron rearrangement similar to the behavior of Ba under strong compression. The special softening of Ce and of Pr at low pressures and the volume collapse transitions observed in both these elements are commonly related to a sudden increase in *f-d* hybridization, and "*f*-electron delocalization," "intermediate valence," and "interconfiguration fluctuation" represent just other terms commonly used to describe the same phenomenon.[72–79] Since similar transitions are assumed to occur in all the other heavier lanthanides but only under higher pressures,[1,79–81] the corresponding anomalies may be reduced quite strongly when the materials are stiffened by the completion of the *s-d* transfer. Whether the transitions to low symmetry structures in Nd and Sm in the upper pressure range of the isothermal (x-ray diffraction) studies[1,80] reflect this more continuous increase in the *f-d* hybridization remains, however, an open question.

Finally, the comparison of Eu and Yb with Ba on the one hand and with the regular lanthanides on the other hand seem to indicate that "divalent" Eu and Yb are both effected already at ambient pressure by some *f*-electron contributions which lead to a clear distinction in the compression behavior with respect to Ba. As the *f-d* electron hybridization increases in Eu and Yb under pressure,[77] a behavior similar to Ce and Pr is approached, and one can speculate, that the extrapolated curves would follow closely the behavior of the strongly *f-d* hybridized trivalent lanthanides. Therefore, an almost continuous transition from a "divalent," weakly *f-d* hybridized to a "trivalent," strongly hybridized situation appears to be conceivable in these two cases.

The final answer to these questions requires, however, further theoretical as well as experimental studies on both the regular and the anomalous lanthanides in the much wider experimental region now accessible with current experimental effort.[82]

ACKNOWLEDGMENTS

Valuable support by the staff of HASYLAB at DESY, Hamburg, and especially by Werner Sievers in Paderborn is gratefully acknowledged. This work was supported in a large part by the German Ministry for Research and Technology (BMFT) under Contract No. 05340AXBO.

---

*Present address: Fachhochschule Offenburg, D-7600 Offenburg, Germany.

[1] T. Krüger, B. Merkau, W. A. Grosshans, and W. B. Holzapfel, High Press. Res. **2**, 193 (1990).

[2] T. Krüger, thesis, Paderborn, 1987.

[3] W. A. Grosshans, thesis, Paderborn, 1987.

[4] T. H. Hall and L. Merrill, Inorg. Chem. **2**, 618 (1963).

[5] P. W. Bridgman, *Collected Experimental Papers* (Harvard University Press, Cambridge, 1964).

[6] D. R. Stephens, J. Phys. Chem. Solids **25**, 423 (1964).

[7] G. J. Piermarini and C. E. Weir, Science **144**, 69 (1964).

[8] C. E. Monfort III and C. A. Swenson, J. Phys. Chem. Solids **26**, 623 (1965).

[9] E. A. Perez-Albuerne, R. L. Clendenen, R. W. Lynch, and H. G. Drickamer, Phys. Rev. **142**, 392 (1966).

[10] D. B. McWhan, P. C. Souers, and G. Jura, Phys. Rev. **143**, 385 (1966).

[11] S. N. Vaidya and G. C. Kennedy, J. Phys. Chem. Solids **31**, 2329 (1970).

[12] S. N. Vaidya and G. C. Kennedy, J. Phys. Chem. Solids **33**, 1379 (1972).

[13] G. C. Kennedy and R. N. Keeler, in *American Institute of Physics Handbook,* edited by D. E. Gray (McGraw-Hill, New York, 1972), pp. 4–38.

[14] L. Liu, W. A. Bassett, and M. S. Liu, Science **180**, 298 (1973).

[15] K. Syassen and W. B. Holzapfel, Solid State Commun. **16**, 533 (1975).

[16] L. Liu, J. Phys. Chem. Solids **36**, 31 (1975).

[17] H. K. Mao, R. M. Hazen, P. M. Bell, and J. Wittig, J. Appl. Phys. **52**, 4572 (1981).

[18] G. S. Smith and J. Akella, J. Appl. Phys. **53**, 9212 (1982).

[19] W. A. Grosshans, Y. K. Vohra, and W. B. Holzapfel, J. Phys. F **13**, L147 (1983).

[20] J. Staun Olsen, S. Streenstrup, and L. Gerward, Phys. Lett. **109A**, 235 (1985).

[21] J. Akella, S. G. Smith, and A. P. Jephcoat, J. Phys. Chem. Solids **49**, 573 (1988).

[22] R. G. Haire, S. Heathman, and U. Benedict, High Press. Res. **2**, 273 (1990).

[23] J. Staun Olsen, S. Streenstrup, L. Gerward, U. Benedict, J, Akella, and G. Smith, High Press. Res, **4**, 366 (1990).

[24] P. L. Schaufelberger and H. Merx, p. 222 in *Proceedings of the 4th International Conference on High Pressure,* Kyoto (1974).

[25] W. H. Zachariasen and F. H. Ellinger, Acta Crystallogr. A **33**, 155 (1976).

[26] S. Endo, H. Sasaki, and T. Mitsui, J. Phys. Soc. Jpn. **42**, 882 (1977).

[27] S. Endo, N. Fujioka, and H. Sasaki, in *High-Pressure Science and Technology,* edited by K. D. Timmerhaus and M. S. Barber (Plenum, New York, 1979), Vol. 1, p. 217.

[28] F. F. Voronov, V. A. Goncharova, and O. V. Stal'gorova, Zh. Eksp. Teor. Fiz. **76**, 1351 (1979) [Sov. Phys. JETP **49**, 687

(1979)].

[29] A. K. Singh, High Temp. High Press. **12**, 47 (1980).

[30] J. Staun Olsen and L. Gerward, High Temp. High Pressures **16**, 515 (1984).

[31] J. Staun Olsen, L. Gerward, U. Benedict, and J.-P. Itie, Physica **133B**, 129 (1985).

[32] K. Syassen and W. B. Holzapfel, in *High-Pressure Science and Technology* (Ref. 27), p. 223.

[33] K. Takemura and K. Syassen, J. Phys. F **15**, 543 (1985).

[34] H. Weik and K. Strnat, in *Landoldt Börnstein* 6, Auflage Band IV 2c (Springer-Verlag, Berlin, 1965), p. 626.

[35] F. H. Spedding, in *CRC Handbook of Chemistry and Physics,* 59th edition, edited by R. C. Weast and M. J. Astle (CRC Press, West Palm Beach, Florida, 1979), p. B261.

[36] J. F. Smith and F. A. Gjevre, J. Appl. Phys. **31**, 645 (1960).

[37] J. R. Stephens and O. Johnson, J. Less-Common Met. **17**, 243 (1969).

[38] J. J. Tonnies, K. A. Gschneidner, Jr., and F. H. Spedding, J. Appl. Phys. **42**, 3275 (1971).

[39] W. H. Gust and E. B. Royce, Phys. Rev. B **8**, 3595 (1973).

[40] E. S. Fisher, M. I. Manghnani, and R. Kikuta, J. Phys. Chem. Solids **34**, 687 (1973).

[41] J. D. Greiner, R. J. Schlitz, Jr., J. J. Tonnies, F. F. Spedding, and J. F. Smith, J. Appl. Phys. **44**, 3862 (1973).

[42] J. D. Greiner, D. M. Schlader, O. D. McMasters, K. A. Gschneidner, Jr., and J. F. Smith, J. Appl. Phys. **47**, 3427 (1976).

[43] R. R. Rao and A. Ramanand, Phys. Status Solidi B **122**, 11 (1984).

[44] L. V. Al'tshuler, A. A. Bakanova, and I. P. Dudoladov, Pis'ma Zh. Eksp. Teor. Fiz. **8**, 193 (1968) [JETP Lett. **8**, 115 (1968)].

[45] W. J. Carter, J. N. Fritz, S. P. Marsh, and R. G. McQueen, J. Phys. Chem. Solids **36**, 741 (1975).

[46] W. B. Holzapfel, in *Molecular Solids Under Pressure,* edited by R. Pucci and G. Piccitto (North-Holland, Amsterdam, 1991), p. 61.

[47] W. B. Holzapfel, High Press. Res. **7**, 290 (1991).

[48] W. B. Holzapfel, Europhys. Lett. **16**, 67 (1991).

[49] K. Syassen and W. B. Holzapfel, Europhys. Conf. Abstr. **1A**, 75 (1975).

[50] W. B. Holzapfel, in *High Pressure Chemistry,* edited by H. Kelm (Reidel, Boston, 1978), p. 177.

[51] W. B. Holzapfel, Deutsches Patent p. 231 2507.7 (1973).

[52] W. B. Holzapfel and W. May, in *High Pressure Research in Geophysics,* edited by S. Akimoto and M. H. Manghnani [Adv. Earth and Planetary Sciences **12**, 73 (1982)].

[53] W. A. Grosshans, E.-F. Düsing, and W. B. Holzapfel, High Temp. High Press. **16**, 539 (1984).

[54] R. A. Forman, G. J. Piermarini, J. D. Barnett, and S. Block, Science **176**, 284 (1972).

[55] J. D. Barnett, S. Block, and G. J. Piermarini, Rev. Sci. Instrum. **44**, 1 (1973).

[56] G. J. Piermarini, S. Block, J. D. Barnett, and R. A. Forman, J. Appl. Phys. **46**, 2774 (1975).

[57] G. J. Piermarini and S. Bloch, Rev. Sci. Instrum. **46**, 973 (1975).

[58] H. K. Mao, P. M. Bell, J. W. Shaner, and D. J. Steinberg, J. Appl. Phys. **49**, 3276 (1978).

[59] B. Johansson and A. Rosengren, Phys. Rev. B **11**, 2836 (1975).

[60] H. L. Skriver, Phys. Rev. B **31**, 1909 (1985).

[61] F. D. Murnaghan, Am. J. Math. **49**, 235 (1937).

[62] Yu. Ya. Boguslavskii, V. A. Goncharova, and G. G. Il'ina, Zh. Eksp. Teor. Fiz. **91**, 1735 (1985) [Sov. Phys. JETP **64**, 1027 (1986)].

[63] R. P. Feynman, N. Metropolis, and E. Teller, Phys. Rev. **75**, 1561 (1949).

[64] W. G. McMillan, Phys. Rev. **111**, 479 (1958).

[65] N. C. Holmes, J. A. Moriarty, G. R. Gathers, and W. J. Nellis, J. Appl. Phys. **66**, 2966 (1989).

[66] H. Olijnyk, thesis, Paderborn, 1985.

[67] H. Olijnyk and W. B. Holzapfel, in *High Pressure Geoscience and Material Synthesis,* edited by H. Vollstädt (Academic Verlag, Berlin, 1988), p. 75.

[68] M. S. Anderson, C. A. Swenson, and D. T. Peterson, Phys. Rev. B **41**, 3329 (1990).

[69] I. V. Svechkarev and A. S. Panfilov, Phys. Status Solidi B **63**, 11 (1974).

[70] D. G. Pettifor, J. Phys. F **7**, 613 (1977).

[71] Y. K. Vohra, S. K. Sikka, and W. B. Holzapfel, J. Phys. F **13**, L107 (1983).

[72] B. Coqblin and A. Blandin, Advan. Phys. **17**, 281 (1968).

[73] R. L. Hirst, Phys. Konden. Mater. **11** 255 (1970).

[74] R. Ramirez and L. M. Falicov, Phys. Rev. B **3**, 1255 (1971).

[75] B. Johansson, Philos. Mag. **30**, 469 (1974).

[76] B. Johansson, J. Phys. F **7**, 877 (1977).

[77] K. Syassen, G. Wortmann, J. Feldhaus, K. H. Frank, and G. Kaindl, Phys. Rev. B **26**, 4745 (1982).

[78] *Valence Instabilities,* edited by P. Wachter and H. Boppart (North-Holland, Amsterdam, 1982).

[79] W. A. Harrison, Phys. Rev. B **29**, 2917 (1984).

[80] W. A. Grosshans and W. B. Holzapfel, J. Phys. (Paris) Colloq. **45**, C8-141 (1984).

[81] U. Benedict, W. A. Grosshans, and W. B. Holzapfel, Physica **144B**, 14 (1986).

[82] A. L. Ruoff, H. Xia, H. Luo, and Y. K. Vohra, Rev. Sci. Instrum. **61**, 3830 (1990).